Original Article

Evaluation of the Treatment Planning and Delivery for Hip Implant Cases on Tomotherapy

Pawan Kumar Singh[1,2], Rohit Verma[1], Deepak Tripathi[3], Sukhvir Singh[4], Manindra Bhushan[5], Lalit Kumar[6], Soumitra Barik[5], Munish Gairola[5]

[1]Department of Physics, Amity Institute of Applied Sciences, Amity University (AUUP), Noida, [2]Department of Radiation Oncology, Vardhman Mahavir Medical College and Safdarjung Hospital, [3]Department of Physics, USAR, Guru Gobind Singh Indraprastha University, East Campus, Delhi, [4]Radiation Safety Group, Institute of Nuclear Medicine and Allied Sciences, Defence Research and Development Organisation, [5]Department of Radiation Oncology and Division of Medical Physics, Rajiv Gandhi Cancer Institute and Research Centre, [6]Department of Radiation Oncology, Max Super Speciality Hospital, New Delhi, India

Abstract

Purpose: The metal present in the implant creates artifacts during the treatment simulation, which impacts the treatment planning and delivery of the prescribed dose to the target and sparing normal tissues. This retrospective study evaluated the uncertainties in the planning and delivery of doses for prosthesis cases with dedicated phantom. **Materials and Methods:** In this retrospective study, 11 patients with a hip prosthesis having cervix carcinoma were selected. Two treatment plans were generated on treatment planning system (TPS) for each case. Plan_No_Res was without any beam restriction, and Plan_exit_only was the plan with restricted beam entry through the metallic implant. An indigenous phantom was utilized to verify the accuracy of the treatment. In the phantom, some groves were present, which could be filled by implants that mimic the patient's geometries, like left, right and bilateral femur implants. The delivered doses were recorded using optically stimulated luminescence dosimeters (OSLDs), which were placed at different positions in the phantom. The plans were further calculated using megavoltage computed tomography (MVCT) scans acquired during treatment. **Results:** The patient data showed no significant dose changes between the two planning methods. The treatment time increases from 412.18 ± 86.65 to 427.36 ± 104.80 with $P = 0.03$ for Plan_No_Res and Plan_exit_only, respectively. The difference between planned and delivered doses of various points across phantom geometries was within ± 9.5% in each case as left, right, and bilateral implant. The variations between OSLDs and MVCT calculated doses were also within ± 10.8%. **Conclusion:** The study showed the competency of tomotherapy planning for hip prosthesis cases. The phantom measurements demonstrate the errors in dosimetry near the implant material, suggesting the need for precise methods to deal with artifact-related issues.

Keywords: Hip prosthesis, megavoltage computed tomography, metallic implant, OSLD, tomotherapy

Received on: 26-12-2023 **Review completed on: 16-02-2024** **Accepted on: 21-02-2024** **Published on: 25-06-2024**

Introduction

Cancer is a deadly disease if not treated in time. Cancer cases are increasing rapidly with the changing lifestyle and environmental conditions such as air pollution, water pollution, and the chemicals used in food items at production and processing units.[1,2] According to a recent census GLOBOCAN 2020, a 13% increase will be observed every 10 years from 2020 to 2040.[3,4] Advanced technologies must be adopted to deal with this cancer burden and complexity in treatment. Carcinoma of the cervix is one of the common pelvis malignancies, and these patients require radiotherapy during their treatment.[5,6] Many old patients go through the metallic implant in the femur because of fracture or bone loss.[7]

Access this article online

Quick Response Code:

Website: www.jmp.org.in

DOI: 10.4103/jmp.jmp_182_23

Patients with implants possess problems during diagnosis and treatment and may require special attention at every treatment stage. The high Z material used for implants interacts with the X-ray beam used for diagnosis and treatment, producing scattering and beam hardening, which causes artifacts in the image.[8] Radiotherapy requires high accuracy and precision to target the tumor and spare the normal organs in the surroundings.[9] The carcinoma (Ca) cervix cases

Address for correspondence: Dr. Pawan Kumar Singh, Department of Radiation Oncology, Vardhman Mahavir Medical College and Safdarjung Hospital, Ministry of Health and F. W., Government of India, New Delhi - 110 029, India.
E-mail: pawansingh786125@gmail.com

How to cite this article: Singh PK, Verma R, Tripathi D, Singh S, Bhushan M, Kumar L, *et al*. Evaluation of the Treatment planning and delivery for hip implant cases on tomotherapy. J Med Phys 2024;49:270-8.

require advanced treatments such as intensity-modulated radiotherapy (IMRT) and image-guided radiotherapy to prevent unnecessary radiation doses to the bladder and rectum.[10]

The tomotherapy Radixact X9 (Radixact X9, Accuray Inc. Sunnyvale, CA) treatment delivery machine has a linear accelerator installed on a slip-ring gantry that can deliver flattening filter-free photon beams in Tomo-Direct, the three-dimensional (3D) conformal radiotherapy form or IMRT in helical form..[11] Dynamic and fixed jaw treatment delivery options are available. Three jaw settings are 40 cm × 1 cm, 40 cm × 2.5 cm, and 40 cm × 5 cm; dynamic jaw options are available for the latter two. The binary multi-leaf collimators (MLCs) have 64 leaves, each having projection of 6.25 mm at the isocenter. Helical treatment delivery involves the couch moving continuously while the ring gantry delivers a modulated fan beam continuously.[12] To guide treatment, 3.2 MV megavoltage computed tomography (MVCT) was on board.

Sibata *et al*.[13] studied the dosimetric influence of hip prosthesis in high-energy photons. They showed the changes in the beam profile due to attenuation caused by implant material. The American Association of Physicists in Medicine Task Group (AAPM TG)-63[14] has recommended the steps for planning and delivery in hip prosthesis cases. In the report,[14] Reft *et al*. suggested avoiding the direct entry of radiation beams through the implant material. Panda *et al*.[10] compared the treatment plans for Halcyon and helical tomotherapy plans for cervix cases and found dosimetrically equivalent results.

In radiotherapy, it is recommended to perform tests on phantoms to find uncertainties; this allows the researcher to explore multiple pathways without harming the patient. Designing a specific phantom for the different cases and performing the essential steps on the phantom provides a clear picture of the challenges faced. Acquah *et al*.[15] used CIRS phantom with metal inserts to study the impact of the artifacts on calculation algorithms. The 3D printing also helps in designing dedicated phantoms for radiotherapy measurements.[16]

This study was designed to find the dosimetric effect of different optimization methods on a patient's treatment plan. The study includes the phantom study for different hip implant cases: right hip, left hip, and bilateral hip implant and the effect of the artifacts on the dose calculation in these cases. The dose delivery on the phantom was recorded using optically stimulated luminescence dosimeters (OSLDs) to validate the treatment planning system (TPS) doses. The MVCT images were reviewed for planning the implant cases.

Materials and Methods

Patient selection and simulation

For this retrospective analysis, a total of 11 patients with hip prostheses who had cervical cancer were selected. The patients were divided into three groups: six for the right implant, three for the left implant, and two for the bilateral implant. The femoral heads ranged in size from 40 to 54 millimeters across. The simulation was performed on a Somatom Sensation Open computed tomography (CT) simulator (Siemens Healthineers, Germany) with 5 mm slice thickness in the head first supine position using thermoplastic immobilization.

Patient contouring and treatment planning

The contouring was done as per the EMBRACE II Study Protocol.[17] Gross tumor volume (GTV) was gross disease visible of T2 magnetic resonance imaging (MRI) which was co-registered to planning CT scan. High-risk CTV included the entire cervix with gross disease as visible on T2 MRI. Low-risk CTV (CTV-LR) included the entire uterus, fallopian tubes, ovaries, parametria, and 2 cm of normal vagina inferior to gross disease. Internal target volume (ITV) was generated by giving 1 cm margin in the superior, anterior, and posterior and 0.5 cm lateral direction to CTV-LR, to account for bladder and rectum motion during treatment. Elective nodal CTV included bilateral common iliac, external iliac, internal iliac, obturator, and presacral nodes. ITV and elective nodal CTV were combined to generate ITV final volume (ITV final). Planning target volume (PTV) was generated by giving 5 mm isotropic margin to ITV final volume. The femur, implanted femur, bladder, rectum, and bowel structures were drawn, and the posterior wall of the bladder (bladder wall) and the anterior wall of the rectum (rectum wall) were also contoured. The dose spillage outside the target was controlled by drawing 3 cm ring around PTV. The Accuray TPS Precision (Accuray Precision 2.0.1.1 [5], Accuray Inc., Sunnyvale, CA) was used to create inverse IMRT plans with a dynamic jaw width of 2.5, a pitch of 0.43, and a modulation factor of 2.5 to optimize the plans. Two plans were created for each patient; the first was optimized without beam path restriction and named Plan_No_Res. The second was optimized for similar objectives and restricted beam entry through the implanted femur, and it was named Plan_exit_only. The plans were optimized to achieve the target dose of 45 Gray (Gy) in 25 fractions. The objectives used for optimization were target PTV: $V_{95\%}$ = 100% dose (desired), V_{45Gy} = 95% dose (acceptable), and D_{max} (point dose) <105% for organs at risk. Bladder: V_{40Gy} <50%, V_{30Gy} <70%, rectum: V_{40Gy} <70%, V_{30Gy} <90%, bowel: V_{45Gy} <120 cc, and Dmax <105%. The plans were calculated using the convolution superposition algorithm with high resolution. Figure 1 shows the isodoses of 95% and 50% for different cases of femur implants.

Patient data evaluation and analysis

The PTV and OARs were assessed using Dose Volume Histograms (DVH). The plan quality was assessed using the following metrics: $D_{95\%}$, $D_{98\%}$, $D_{2\%}$, and $V_{95\%}$ of PTV. Furthermore, an estimate of the gradient index was also calculated. $D_{0.1cc}$, mean dose (Dmean), V_{30Gy}, and V_{40Gy} were estimated from the dosimetric data for the bladder and rectum, while $D_{0.1cc}$, D_{1cc}, D_{2cc}, D_{5cc}, V_{10Gy}, V_{20Gy}, V_{35Gy}, and Dmean were estimated for the bladder and rectum walls. $D_{0.1cc}$, Dmean,

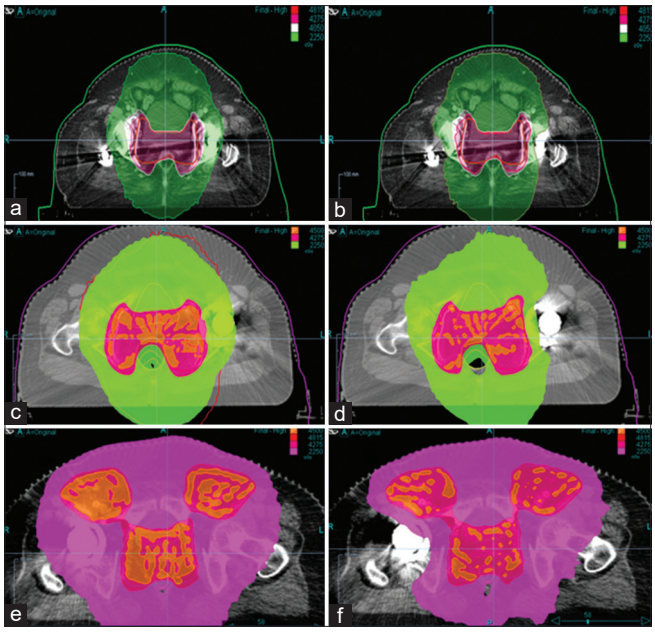

Figure 1: The dose distributions of the 95% and 50% isodose colour wash for various cases of femur implant were: (a) and (b) represent the right femur implant. (c) and (d) depict the isodose lines for the left femur implant. (e) and (f) show the isodoses for bilateral femur implants. (a), (c) and (e) correspond to the plans with beam entry through the implant, while (b), (d), and (f) correspond to plans without beam entry through the implant

V_{35Gy}, V_{40Gy}, and V_{45Gy} were computed for the Bowel. Along with these parameters, treatment time was also calculated. $D_{x\,cc}$ signifies the dose received by organ in x cc volume, and $D_{x\,\%}$ signifies the dose received by organ in x % of volume. $V_{x\,Gy}$ signifies the volume of organ received x Gy dose, and V x % signifies the volume of organ received x % of dose. The gradient index (GI) is the ratio of the volume of 50% of the prescription isodose to the volume of the prescription isodose 95%.[18] The formula used for GI was denoted as gradient.

$$\text{Gradient} = \frac{\text{Volume of Isodose Receiving 50\% Dose}}{\text{Volume of Isodose Receiving 95\% Dose}}$$

Phantom design

The study was conducted with a cylindrical phantom with a length of 21 cm and a diameter of 20 cm. The phantom consisted of perspex material with three grooves for inserting implant rods. Two stainless steel inserting rods with a mass density of 7.5 8 g/cc were used to mimic the implants. The lengths of the rods were 20.9 cm and 22.5 cm, respectively, with 2.1 cm diameter. The third inserting rod, hollow poly vinyl chloride (PVC) pipe with a wall thickness of 2 mm, length of 22 cm and diameter of 2 cm filled with wax, was used to simulate normal bone tissue shown in Figure 2a. A rectangular block (L = 20 cm, width = 6.5 cm, height = 12.2 cm) with multiple detachable layers was in the middle of the phantom shown in Figure 2c, the ionization chamber CC13 at 6.7 cm depth. We also placed OSLDs in different planes to stimulate the bladder, bladder wall, rectum wall, and rectum. The OSLDs were kept in grooves created on a 1 mm wax sheet shown in Figure 2b. Figure 2d demonstrates the typical geometry of the different layers in phantom. The phantom was scanned on a CT simulator in pelvis protocol with a 1 mm slice thickness using the same CT simulator. Figure 2e shows the CT axial view of the right femur implant in the phantom. Three different scans were performed to denote bilateral and unilateral scans. We imported all the scans to the Accuray precise contouring station. We contoured the chamber volume and named it GTV, and the margin to it was the PTV. The different layers were also contoured and named bladder, bladder wall, rectum wall, and rectum. The bladder and rectum contours were shaped as the actual clinical structures. Figure 2g shows the 3D view of the phantom in TPS.

Treatment planning and dose delivery for phantom

Each implant set, such as the bilateral, left, and right implants, had two distinct plans. All the plans were generated with dynamic jaws 2.5 cm × 40 cm, 0.43 pitch, and a modulation factor of 2.5 for the dose of 45Gy in 25 fractions utilizing helical IMRT technique. The plans were calculated with a convolution superposition algorithm in high resolution. The plans that did not restrict beam entry through implants were labeled with the suffix_No_Res, while those that did restrict beam entry and only permit radiation beam exit were labeled with the suffix Exit_Only. The plans had the following names: IM_R_No_Res and IM_R_Exit_Only for the right implant and IM_L_No_Res and IM_L_Exit_Only for the left implant. Bl_No_Res and Bl_Exit_Only were utilized for bilateral implants. The plans were delivered to the phantom aligned with moving laser red lasers used for patient setup, and an MVCT scan was performed to ensure the phantom positioning. Figure 2f shows the axial view of the MVCT scan of the phantom. After applying shifts to the chamber and implants, the treatment was performed. Figure 3 illustrates the dose distributions of the 95% isodose and 50% isodose for various cases of femur implant in the phantom. (a) and (b) depict bilateral femur implant cases, (c) and (d) demonstrate the isodose for the left femur implant. (e) and (f) represent the isodoses for the right femur implant. In which 3((a), (c),(e)) correspond to the plans with beam entry through the implant, while 3((b), (d),(f))correspond to plans without beam entry through the implant.

Dosimetry instruments

The OSLDs used were BeO elements of dimensions 4.65 mm × 4.65 mm × 0.5 mm from RadPro International GmbH (Freiberg Instruments GmbH, Freiberg, Germany). The element was covered in a black-colored sheath of Acrylnitril-Butadien-Styrol-Copolymer. An average of 5 chips were placed in each plane to measure the doses. These chips were contoured in the simulation CT to obtain the mean doses calculated from TPS to the chip. A total of 21 OSLD chips were in each set of measurements. The OSLDs were read using light-emitting diodes of 460 nm wavelength light.

The point doses were measured using the ionization chamber CC13 (0.13 cc) (IBA Dosimetry, Germany) with a Wellhofer

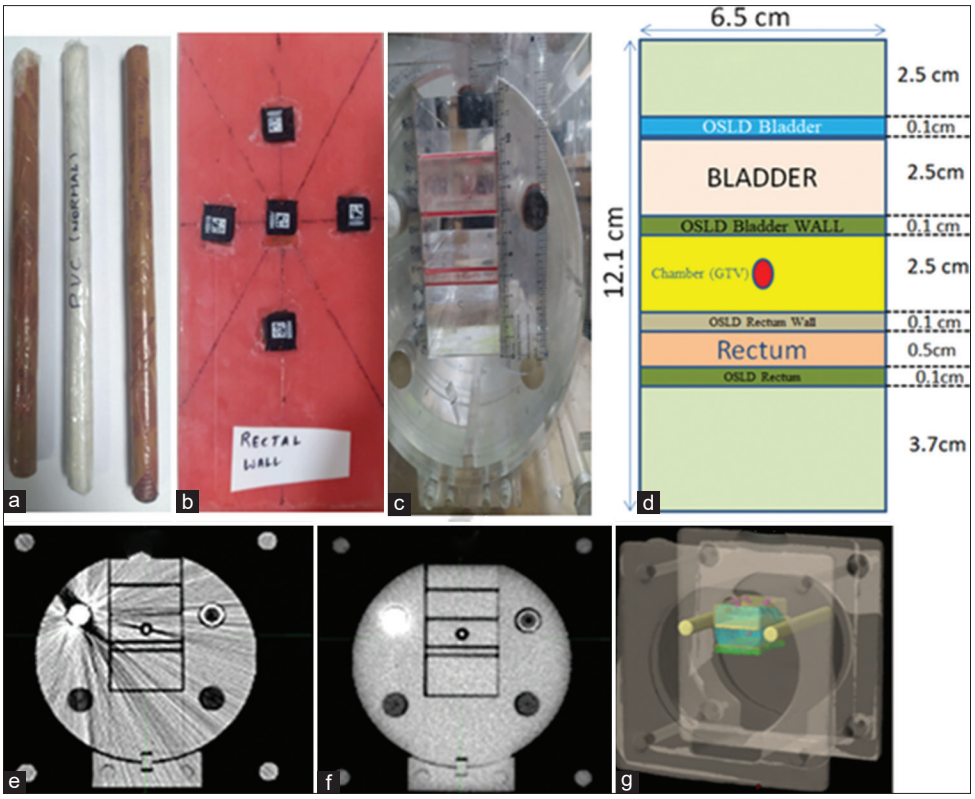

Figure 2: (a) The rods used for implant. (b) The placement of OSLDs in a layer. (c) Photograph of the phantom in axial plan. (d) The overall geometry of the different layers in phantom. (e) The computed tomography axial view of the right femur implant in the phantom. (f) The axial view of the megavoltage computed tomography scan of the phantom. (g) The three-dimensional-view of the phantom in treatment planning system

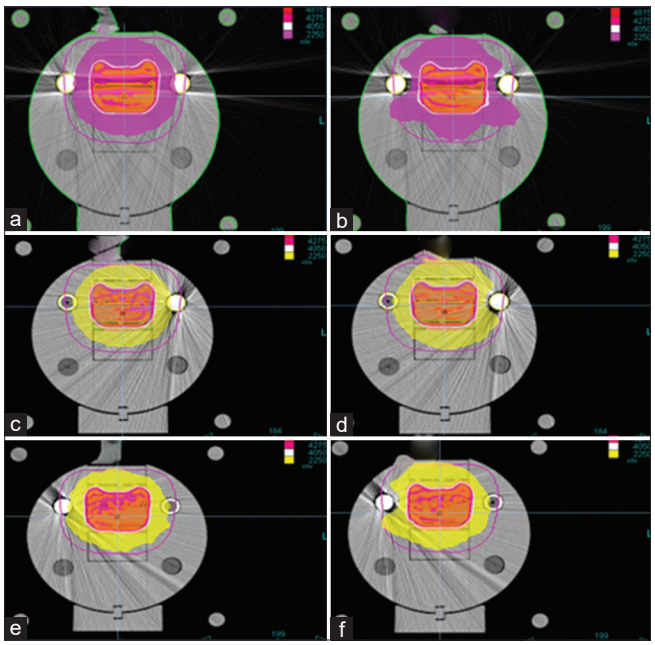

Figure 3: The dose distributions of the 95% isodose and 50% isodose for various cases of femur implant in the phantom, were (a) and (b) depict bilateral femur implant cases, (c) and (d) demonstrate the isodose for the left femur implant. (e) and (f) represent the isodoses for the right femur implant. In which 3((a), (c),(e)) correspond to the plans with beam entry through the implant, while 3((b), (d),(f))correspond to plans without beam entry through the implant

Dose-1 electrometer. The chamber was at the center of the target.

Megavoltage computed tomography dose calculation

The MVCT images acquired during plan implementation were imported to the Mim software (MIM, version 7.1.90, Mim software Inc., Beachwood, OH, United States) of the precise ART module. This module enables the registration of the planning CT images and the MVCT images. The structures in the planning images get transferred to the MVCT images, and we can evaluate the differences between planned and delivered doses. The MVCT calibration curve was uploaded to this software, and applying the curve, we calculated the doses to the different structures present in CT. Figure 4 compares computed tomography (CT) and megavoltage computed tomography (MVCT) images alongside dose difference: (a) and (b) display images for bilateral implants. (c) and (d) showcase images of the left femur implant. (e) and (f) represent images for the right femur implant. Where 4((b), (d), and (f) correspond to the calculated dosage on MVCT pictures, while 4((a), (c), and (e)) reflect the dose distribution on CT images.

All computational statistics were performed with statistical analysis in Python software (Spyder IDE version 5.1.5, Raybaut, P.[19] The paired t-test was used to analyze the difference in dosimetric parameters, and a P-value ≤ 0.05 was considered statistically significant. The Microsoft Office

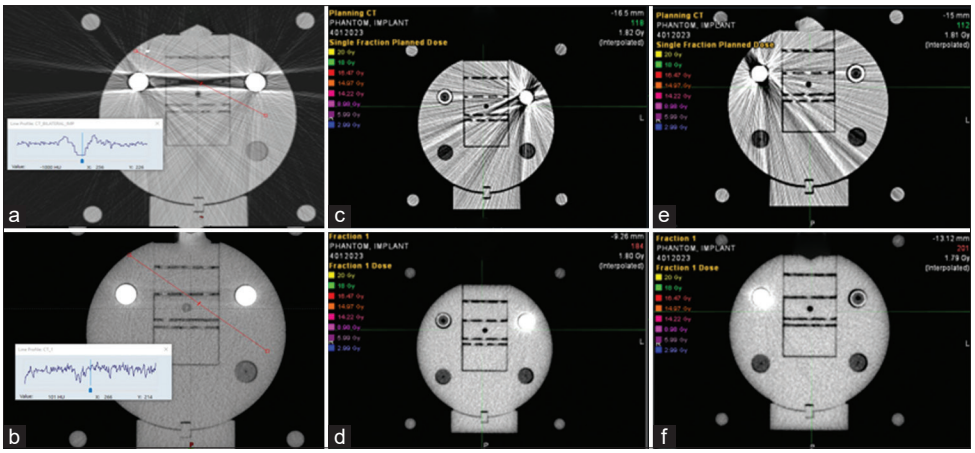

Figure 4: The comparison between computed tomography and megavoltage computed tomography (MVCT) images and their respective noise levels: (a and b) for bilateral implant, (c and d) for the left femur, and (e and f) for the right femur implant. The reduced noise levels in MVCT images (b), (d), and (f) highlight their superiority over the CT images (a), (c), and (e)

Excel sheets were used to calculate the % differences, mean, and standard deviation.

Results

Dosimetric analysis for patients

The patient's planning data are documented in Table 1. The two plans Plan_No_Res and Plan_exit_only were compared using the dose-volume histogram (DVH) data, and there was no significant variation in PTV dosimetry parameters, i.e., $V_{95\%}$ ($P = 0.39$), $D_{95\%}$ ($P = 0.24$), $D_{2\%}$ ($P = 0.29$), and $D_{98\%}$ ($P = 0.27$). Similarly, the organ-at-risk (OAR) doses and GI were comparable in both the planning techniques with $P > 0.05$ for all the dosimetric parameters evaluated for the bladder, bladder wall rectum, and rectum wall. There was a significant increase in treatment time from 412.18 ± 86.65 to 427.36 ± 104.80 with $P = 0.03$ for Plan_No_Res and Plan_exit_only, respectively.

Dosimetric analysis for Phantom

Table 2 summarizes the TPS and OSLDs received and calculated MVCT average point doses for both No_Res and Exit_Only plans. Detailed measurements for various marked points in the Phantom were provided in Supplementary Table.

Bilateral femur implant case: The average difference between OSLD received and TPS calculated dose in No_Res plans for the Bladder was 3.53%, for the bladder wall was -6.53% and -1.67% and 4.31% for the rectum and rectum wall respectively. In Exit_Only plans, the dose differences were 5.44%, 7.46%, 3.46% and 4.35% for the Bladder, Bladder wall, Rectum and Rectum wall, respectively. The dose difference between OSLD received and calculated on MVCT doses in No_Res plans were 5.35%, -1.71%, 3.52% and 10.80% for the Bladder, bladder wall, rectum and rectum wall, respectively. Similarly, 6.04%, 6.29%, 4.40%, and 5.04% were for Bladder, bladder wall, rectum, and rectum wall, respectively, in Exit_only Plans.

Left femur implant point: The average difference between OSLD received and TPS calculated dose in No_Res plans, for the Bladder, bladder, rectum, and rectum wall were 4.49%, 2.56%, 5.84%, and 2.96%, respectively. For Exit_Only plans, these discrepancies were 9.37%, 2.7%, -0.14%, and 3.02%, respectively. The difference between OSLD received and calculated on MVCT doses in No_Res plans were 5.77%, 4.70%, 8.0%, and 5.27% for the Bladder, bladder wall, rectum, and rectum wall, respectively. In Exit_Plans, these differences were 9.91%, 3.56%, 1.36%, and 4.31%, respectively.

Right Femur Implant: The average difference between OSLD received and TPS calculated dose in No_Res plans, for the Bladder, bladder wall, rectum, and rectum wall were 2.88%, -5.92%, 1.85%, and -0.17%, respectively. Meanwhile, for Exit_Only plans, these discrepancies stood at 3.43%, 1.27%, 3.47%, and 1.92%, respectively. Regarding the difference between OSLD received and calculated on MVCT doses, in No_Res plans was 4.38%, -2.77%, 4.49%, and 2.84% for the Bladder, bladder wall, rectum, and rectum wall, respectively. For Exit_Plans, these differences were 4.36%, 2.43%, 4.91% and 3.62% respectively.

Point dose measurements

Table 3 illustrates the disparity in dose between the measured values by the ion-chamber and the TPS-calculated doses for all bilateral, left femur implant, and right implant cases in both NO_Res and Exit_Only plans. The variations were within ± 2%.

Discussion

The tomotherapy planning and delivery system is different from the C-linac. The fan beam of radiation was used to deliver the dose in a helical pattern. The patient dosimetry data showed no significant dose changes between the two planning methods. Our previous study derived similar results when the patients were planned for the Clinac-ix 2300-CD. Singh *et al*. concluded that the beam avoidance required for the volumetric-modulated arc therapy (VMAT) plans was not significant in the planning of hip prosthesis cases.[20] David *et al*.[21] different VMAT

Table 1: Patient treatment plan data and plan comparisons

Structure	Parameter	Planning technique (mean±SD)		*P*
		Plan_No_Res	Plan_exit_only	
PTV	V_{95} (%)	99.13±0.52	99.17±0.52	0.39
	D_{95} (cGy)	4448.73±29.47	4442.73±31.01	0.24
	D_{2} (%)	4554.64±16.96	4535.45±62.34	0.29
	D_{98} (%)	4383.36±58.99	4404.27±72.45	0.27
Bladder	V_{40Gy} (%)	48.81±5.96	49.467±6.29	0.12
	V_{30Gy} (%)	82.55±16.25	83.9±14.64	0.59
	$D_{0.1cc}$ (cGy)	4625±49.97	4612.09±27.22	0.23
	D_{mean} (cGy)	3785.55±160.33	3812.91±176.86	0.39
Bladder wall	V_{10Gy} (%)	100	100	
	V_{20Gy} (%)	99.32±1.43	98.84±2.13	0.25
	V_{35Gy} (%)	69.30±9.12	73.16±10.35	0.15
	$D_{0.1cc}$ (cGy)	4594.36±29.92	4591.82±24.81	0.72
	$D_{1.0cc}$ (cGy)	4559.18±23.97	4558.27±16.46	0.87
	$D_{2.0cc}$ (cGy)	4545.27±19.72	4546.18±13.6	0.83
	$D_{5.0cc}$ (cGy)	4526.0±15.5	4526±15.5	0.93
	D_{mean} (cGy)	3910.27±141.1	3921.09±123.25	0.69
Rectum	V_{40Gy} (%)	48.84±10.60	50.9±10.2	0.20
	V_{30Gy} (%)	79.06±8.3	81.71±9.98	0.45
	$D_{0.1cc}$ (cGy)	4635.64±45.90	4643.09±60.17	0.58
	D_{mean} (cGy)	3965.45±324.89	3731.91±329.43	0.49
Rectum wall	V_{10Gy} (%)	96.39±10.74	96.38±10.74	0.34
	V_{20Gy} (%)	94.65±11.89	93.48±11.90	0.28
	V_{35Gy} (%)	65.04±7.22	66.85±7.29	0.34
	$D_{0.1cc}$ (cGy)	4627.45±45.57	4629.45±58.58	0.88
	$D_{1.0cc}$ (cGy)	4565.45±23.49	4566.73±31.76	0.86
	$D_{2.0cc}$ (cGy)	4537.55±31.16	4542.27±25.14	0.53
	$D_{5.0cc}$ (cGy)	4501.09±23.51	4499.18±26.7	0.58
	D_{mean} (cGy)	3684.55±378.19	3717.27±387.45	0.49
Bowel	V_{45Gy} (cc)	36±56.73	37.38±61.61	0.65
	V_{40Gy} (cc)	160.21±143.04	154.64±146.81	0.44
	V_{35Gy} (cc)	307.13±154.63	249.13±154.63	0.35
	$D_{0.1cc}$ (cGy)	4560±75.01	4540.64±61.96	0.12
	D_{mean} (cGy)	2057.73±378.63	2028.09±389.31	0.22
Gradient		3.07±0.33	3.05±0.30	0.84
Treatment time (s)		412.18±86.65	427.36±104.80	0.03

SD: Standard deviation

planning strategies for bilateral hip prostheses for the prostate and concluded that the optimizer-constrained methods were sparing the oars in an improved manne. Prabhakar *et al*. studied beam avoidance using two arcs in VMAT plans for a bilateral hip prosthesis in prostate cases, and they found the constrained methods helpful in respecting doses toward the implant.[22]

Parenica *et al*.[23] used full arc to optimize the VMAT plans without any avoidance and with the Mote Carlo calculation methods found better plan quality for hip prosthesis prostate cancer cases. In this study, the results did not indicate the avoidance of the implanted material. The small increase in the treatment time was the only concern with the plans used the avoidance. Therefore, except for the treatment time, the avoidance method can be well recommended because it avoids the uncertainties related to calculation algorithms. There were Monte Carlo studies[24] which show the variation in data due to the presence of metal implants.

In the tomotherapy plans, the optimizer had increased freedom due to the high gantry rotational speed, constant couch movement, and pneumatically moving binary MLCs. These helped to get plans without any significant variation in the gradients of the two different optimization methods. The significant variation in the treatment time was due to the restricted entry of the beam; the gantry had to take multiple rotations to cover the same area because of the constant speed of the couch. According to the AAPM TG-63, the entry of radiation beam through the implanted material should be avoided to avoid uncertainties in the treatment planning of the patients.

The phantom study was required to understand the dosimetric uncertainties in hip prosthesis cases; the present study includes all three possibilities of the implant in the femoral region. The end-to-end test simulating the actual scatter conditions provided clearer insight into these cases. Kumar[25] studied the end-to-end test on tomotherapy for planning bilateral implant cases and concluded that the avoidance methods less affected the helical IMRT plans.[26] Furuya *et al.* studied the spine SBRT cases for spine metal implants and were able to get the results with uncertainties within ± 5% among five different institutes. Gurjar *et al*.[27] highlighted the dose perturbations due to scattering from high-density bone material at bone tissue interface. Further, high-density material causes significant attenuation of the incident radiation beam, which leads to the dose perturbation in the shadow region and gives rise to a dose peak up streaming from the material surface due to backscattering.

The phantom study results showed significant discrepancies when compared with the OSLDS, TPS, and MVCT calculated doses. The OSLD measurements were up to ± 10% from the TPS and the MVCT doses. The OSLDs were distributed in the phantom such that it covered all the measure junctions of the target and OARs, the bladder wall and rectum wall were present in the target region, and the bladder and rectum OSLDS were giving an overview of the OAR doses. OSLDs were reliable dosimeters for photon dosimetry,[28,29] and BeO used in the study had tissue equivalence and could detect smaller doses too.[30] They used the alkaline dosimeters to study the dose uncertainties in the planning and delivery of human cadavers having metallic implants inside; they marked the variation in doses up to 33% between planned and delivered. In this study, the differences in planned doses within the target region and measured using an ionization chamber, were found to be within ± 2%. However, discrepancies observed at various points through OSLD raised concerns and warrant comprehensive evaluation from all angles. One possible explanation for these variations could be the presence of interface scattered photons near metallic implants.

The MVCT images and the dose calculation could be a better option for planning hip prosthesis cases. The phantom CT scan

Table 2: Dosimetric comparison of optically stimulated luminescence and treatment planning system calculated doses, optically stimulated luminescence, and megavoltage computed tomography calculated dose

Case	Position	IM_No_Res						OSLD Doses cGy (D)	IM_Exit Only				
		OSLD Doses cGy (A)	Planned (TPS) Doses cGy (B)	MVCT Doses cGy (C)	OSLD vs Planned Dose % Difference (A-B)	OSLD vs MVCT Dose % Difference (A-C)	Planned vs MVCT Dose % Difference (B-C)		Planned (TPS) Doses cGy (E)	MVCT Doses cGy (F)	OSLD vs Planned Dose % Difference (D-E)	OSLD vs MVCT Dose % Difference (D-F)	Planned vs MVCT Dose % Difference (E-F)
Left Femur Implant	Bladder	131.32±13.54	125.04±9.23	123.33±8.83	4.49	5.77	1.35	147.90±11.34	133.61±6.15	132.83±6.41	9.37	9.91	0.59
	Bladder Wall	185.00±4.94	180.16±0.11	176.20±0.84	2.56	4.7	1.39	186.96±20.52	179.99±0.25	178.40±0.55	2.7	3.56	0.88
	Rectum Wall	187.15±8.56	181.31±1.80	177.00±1.87	2.96	5.27	2.38	186.79±6.64	181.01±1.76	178.60±1.67	3.02	4.31	1.33
	Rectum	160.04±3.28	150.66±2.44	147.20±2.59	5.84	8	2.3	151.45±6.71	151.47±2.41	149.20±2.05	-0.14	1.36	1.5
Right Femur Implant	Bladder	132.78±15.55	126.99±10.47	125.00±10.46	2.88	4.38	1.58	132.12±6.90	127.58±8.04	126.33±7.65	3.43	4.36	0.96
	Bladder Wall	173.32±23.92	180.18±0.08	174.80±1.10	-5.92	-2.77	2.98	182.43±6.95	179.91±0.26	177.80±0.45	1.27	2.43	1.17
	Rectum Wall	180.56±7.70	180.61±0.83	175.20±0.84	-0.17	2.84	2.95	184.92±7.74	181.14±1.23	178.00±1.00	1.92	3.62	1.73
	Rectum	162.34±5.76	159.28±4.29	155.00±4.36	1.85	4.49	2.69	156.21±5.17	150.63±1.29	148.40±1.14	3.47	4.91	1.48
Bilateral Femur Implant	Bladder	131.45±15.42	125.44±6.95	123.00±6.30	3.53	5.35	1.92	141.43±5.51	133.67±6.33	132.83±5.98	5.44	6.04	0.62
	Bladder Wall	171.79±22.75	179.83±0.21	172.00±1.00	-6.33	-1.71	4.36	192.98±3.40	178.53±1.12	180.80±1.79	7.46	6.29	-1.28
	Rectum Wall	189.40±2.78	181.20±1.13	169.00±12.88	4.31	10.8	6.71	189.76±9.87	181.10±0.83	179.80±0.84	4.35	5.04	0.72
	Rectum	148.36±5.02	150.70±0.87	143.00±6.75	-1.67	3.52	5.12	155.78±5.58	150.27±1.24	148.80±1.30	3.46	4.4	0.38

Table 3: Chamber point dose measurement details in target

Case	No_Res Plans			Exit Only Plans		
	Ion Chamber Measured Doses cGy (A)	Planned (TPS) Doses cGy (B)	Measured vs Planned Dose %Difference (A-B)	Ion Chamber Measured Doses cGy (D)	Planned (TPS) Doses cGy (E)	Measured vs Planned Dose %Difference (D-E)
Left Femur Implant	179.47	181	-0.85	178.95	181.64	-1.5
Right Femur Implant	177.98	180.36	-1.36	180.1	180.68	-0.32
Bilateral Femur Implant	181.95	181	0.52	182.64	179.44	1.75

and MVCT scan show a significant reduction in image streak artifact. The physics of the photoelectric effect helped to reduce the image artifact and to produce an image set without much compromised-on organ and target visualization due to energy ranging 3 MV.[31-33] These studies suggest the use of MVCT images and their benefits in the treatment planning of cases having a metallic implant. Therefore, the use of MVCT images for planning hip prosthesis cases could be an option. The dose contributions measured for MVCT alone for different phantom settings ranged from 2cGy to 3.5cGy which were well within 5% of the prescription dose 180 cGy.[34,35]

The limitations of this study were the unavailability of the metal artifact reduction software and the clinical correlation of the dosimetric data.[36-40] These studies describe the benefits of using artifact reduction algorithms in the case of metal implants.[41] Fischer and Hoskin studied the gastrourinary and gastrointestinal toxicity induced in prostate patients having hip implants; they concluded that VMAT improves the DVH quality. The use of artifact reduction software and clinical data can improve the weightage of the recommendations made in this study.

Conclusion

The study showed the competency of tomotherapy planning for hip prosthesis cases. The optimization methods provided comparable results; to avoid the hidden uncertainties, the beam avoidance optimization method should be considered. The phantom measurements demonstrate the errors in dosimetry near the implant material, suggesting the need for more precise methods to deal with the artifacts. The MVCT image quality and the associated optimization and calculation methods make it an alternative for the planning of hip prosthesis cases.

Acknowledgments

We would like to acknowledge Mr. Deepak Arora, consultant medical physicist (Midas India, New Delhi, India), for providing the phantom, which was modified by the authors for this study. We also thank the management of Rajiv Gandhi Cancer Institute and Research Centre for allowing us to conduct the research work.

Financial support and sponsorship

Nil.

Conflicts of interest

There are no conflicts of interest.

References

1. Manisalidis I, Stavropoulou E, Stavropoulos A, Bezirtzoglou E. Environmental and health impacts of air pollution: A review. Front Public Health 2020;8:14.
2. Anand P, Kunnumakkara AB, Sundaram C, Harikumar KB, Tharakan ST, Lai OS, *et al.* Cancer is a preventable disease that requires major lifestyle changes. Pharm Res 2008;25:2097-116.
3. Global Cancer Observatory. Available from: https://www.gco.iarc.fr/. [Last accessed on 2022 Jan 12].
4. Siegel RL, Miller KD, Wagle NS, Jemal A. Cancer statistics, 2023. CA Cancer J Clin 2023;73:17-48.
5. Yadav G, Bhushan M, Dewan A, Saxena U, Kumar L, Chauhan D, *et al.* Dosimetric influence of photon beam energy and number of arcs on volumetric modulated arc therapy in carcinoma cervix: A planning study. Rep Pract Oncol Radiother 2017;22:1-9.
6. Kumar L, Yadav G, Raman K, Bhushan M, Pal M. The dosimetric impact of different photon beam energy on RapidArc radiotherapy planning for cervix carcinoma. J Med Phys 2015;40:207-13.
7. Guise TA. Bone loss and fracture risk associated with cancer therapy. Oncologist 2006;11:1121-31.
8. Spadea MF, Verburg JM, Baroni G, Seco J. The impact of low-Z and high-Z metal implants in IMRT: A Monte Carlo study of dose inaccuracies in commercial dose algorithms. Med Phys 2014;41:011702.
9. Falcinelli L, Palumbo I, Radicchia V, Arcidiacono F, Lancellotta V, Montesi G, *et al.* Prostate cancer: Contouring target and organs at risk by kilo voltage and megavoltage CT and MRI in patients with and without hip prostheses. Br J Radiol 2015;88:20150509.
10. Panda S, Swamidas J, Chopra S, Mangaj A, Fogliata A, Kupelian P, *et al.* Treatment planning comparison of volumetric modulated arc therapy employing a dual-layer stacked multi-leaf collimator and helical tomotherapy for cervix uteri. Radiat Oncol 2020;15:22.
11. Mackie TR. History of tomotherapy. Phys Med Biol 2006;51:R427-53.
12. Kraus KM, Kampfer S, Wilkens JJ, Schüttrumpf L, Combs SE. Helical tomotherapy: Comparison of Hi-ART and radixact clinical patient treatments at the technical university of Munich. Sci Rep 2020;10:4928.
13. Sibata CH, Mota HC, Higgins PD, Gaisser D, Saxton JP, Shin KH. Influence of hip prostheses on high energy photon dose distributions. Int J Radiat Oncol Biol Phys 1990;18:455-61.
14. Reft C, Alecu R, Das IJ, Gerbi BJ, Keall P, Lief E, *et al.* Dosimetric considerations for patients with HIP prostheses undergoing pelvic irradiation. Report of the AAPM radiation therapy committee task group 63. Med Phys 2003;30:1162-82.
15. Acquah GF, Kyeremeh PO, Hasford F, Boadu M, Sosu EK, Inkoom S. Evaluation of metallic implant artifact on photon beam calculation algorithms using a CIRS thorax phantom. Journal of Radiation Research and Applied Sciences 2018;11:347-9.
16. Tino R, Yeo A, Leary M, Brandt M, Kron T. A systematic review on 3D-printed imaging and dosimetry phantoms in radiation therapy. Technol Cancer Res Treat 2019;18:1533033819870208.
17. Pötter R, Tanderup K, Kirisits C, de Leeuw A, Kirchheiner K, Nout R, *et al.* The EMBRACE II study: The outcome and prospect of two decades of evolution within the GEC-ESTRO GYN working group and the EMBRACE studies. Clin Transl Radiat Oncol 2018;9:48-60.
18. Paddick I, Lippitz B. A simple dose gradient measurement tool to complement the conformity index. J Neurosurg 2006;105 Suppl: 194-201.

19. Raybaut, P. Spyder-documentation. 2009. Available from: https://pypi.org/ or https://pythonhosted.org/ was visited. [Last accessed on 2024 Jun 05].
20. Singh PK, Tripathi D, Singh S, Bhushan M, Kumar L, Raman K, *et al.* To study the impact of different optimization methods on intensity-modulated radiotherapy and volumetric-modulated arc therapy plans for hip prosthesis patients. J Med Phys 2022;47:262-9.
21. To D, Xhaferllari I, Liu M, Liang J, Knill C, Nandalur S, *et al.* Evaluation of VMAT planning strategies for prostate patients with bilateral hip prosthesis. Technol Cancer Res Treat 2021;20:15330338211038490.
22. Prabhakar R, Kumar M, Cheruliyil S, Jayakumar S, Balasubramanian S, Cramb J. Volumetric modulated arc therapy for prostate cancer patients with hip prosthesis. Rep Pract Oncol Radiother 2013;18:209-13.
23. Parenica HM, Mavroidis P, Jones W, Swanson G, Papanikolaou N, Stathakis S. VMAT optimization and dose calculation in the presence of metallic hip prostheses. Technol Cancer Res Treat 2019;18:1533033819892255.
24. Mahuvava C, Du Plessis FC. Dosimetry effects caused by unilateral and bilateral hip prostheses: A Monte Carlo case study in megavoltage photon radiotherapy for computed tomography data without metal artifacts. J Med Phys 2018;43:236-46.
25. Kumar SP. To study the Multimodality End-to-end Testing for Bilateral Metallic Implant in Pelvis. Turk J Oncol 2023;38:333-41. doi: 10.5505/tjo.2023.3892.
26. Furuya T, Lee YK, Archibald-Heeren BR, Byrne M, Bosco B, Phua JH, *et al.* Evaluation of multi-institutional end-to-end testing for post-operative spine stereotactic body radiation therapy. Phys Imaging Radiat Oncol 2020;16:61-8.
27. Gurjar OP, Mishra SP, Bhandari V, Pathak P, Patel P, Shrivastav G. Radiation dose verification using real tissue phantom in modern radiotherapy techniques. J Med Phys 2014;39:44-9.
28. Ispir EB, Sarigul N, Yegingil Z. NanoDot™ OSLDs in verifying radiotherapy dose calculations in the presence of metal implants: A Monte Carlo assisted research. Radiat Phys Chem 2021;187. [doi: 109577. 10.1016/j.radphyschem.2021.109577].
29. Pradhan AS, Lee JI, Kim JL. Recent developments of optically stimulated luminescence materials and techniques for radiation dosimetry and clinical applications. J Med Phys 2008;33:85-99.
30. Le Fèvre C, Brinkert D, Menoux I, Kuntz F, Antoni D, El-Bitar Z, *et al.* Effects of a metallic implant on radiotherapy planning treatment-experience on a human cadaver. Chin Clin Oncol 2020;9:14.
31. Newhauser WD, Giebeler A, Langen KM, Mirkovic D, Mohan R. Can megavoltage computed tomography reduce proton range uncertainties in treatment plans for patients with large metal implants? Phys Med Biol 2008;53:2327-44.
32. Korol RM, Surry K, Davidson MT, Yartsev S, Rodrigues G, D'Souza DP. Three-dimensional image-based planning for cervix brachytherapy with bilateral hip prostheses: A solution using MVCT with helical tomotherapy. Brachytherapy 2010;9:278-81.
33. Sterzing F, Kalz J, Sroka-Perez G, Schubert K, Bischof M, Roder F, *et al.* Megavoltage CT in helical tomotherapy – Clinical advantages and limitations of special physical characteristics. Technol Cancer Res Treat 2009;8:343-52.
34. De Marco P, Abdi Osman I, Castellini F, Ricotti R, Leonardi MC, Miglietta E, *et al.* Image quality and dose evaluation of MVCT Tomotherapy acquisitions: A phantom study. Phys Med 2019;57:200-6.
35. Mege JP, Wenzhao S, Veres A, Auzac G, Diallo I, Lefkopoulos D. Evaluation of MVCT imaging dose levels during helical IGRT: Comparison between ion chamber, TLD, and EBT3 films. J Appl Clin Med Phys 2016;17:143-57.
36. Puvanasunthararajah S, Fontanarosa D, Wille ML, Camps SM. The application of metal artifact reduction methods on computed tomography scans for radiotherapy applications: A literature review. J Appl Clin Med Phys 2021;22:198-223.
37. Giantsoudi D, De Man B, Verburg J, Trofimov A, Jin Y, Wang G, *et al.* Metal artifacts in computed tomography for radiation therapy planning: Dosimetric effects and impact of metal artifact reduction. Phys Med Biol 2017;62:R49-80.
38. Stradiotti P, Curti A, Castellazzi G, Zerbi A. Metal-related artifacts in instrumented spine. Techniques for reducing artifacts in CT and MRI: State of the art. Eur Spine J 2009;18 Suppl 1:102-8.
39. Shen ZL, Xia P, Klahr P, Djemil T. Dosimetric impact of orthopedic metal artifact reduction (O-MAR) on Spine SBRT patients. J Appl Clin Med Phys 2015;16:106-16.
40. Kubo Y, Ito K, Sone M, Nagasawa H, Onishi Y, Umakoshi N, *et al.* Diagnostic value of model-based iterative reconstruction combined with a metal artifact reduction algorithm during CT of the oral cavity. AJNR Am J Neuroradiol 2020;41:2132-8.
41. Fischer AM, Hoskin PJ. Radiotherapy-induced toxicity in prostate cancer patients with hip prostheses. Radiat Oncol 2022;17:9.

Supplementary Table: Dose comparisons at different points in the bilateral phantom setup, OSL doses and TPS doses, OSL doses and MVCT calculated doses.

Case	Position	IM_No_Res						IM_Exit Only					
		OSLD Doses cGy (A)	Planned (TPS) Doses CGy (B)	MVCT Doses cGy (C)	OSLD vs Planned Dose % Difference (A-B)	OSLD vs MVCT Dose % Difference (A-C)	Planned vs MVCT Dose % Difference (B-C)	OSLD Doses cGy (D)	Planned (TPS) Doses CGy (E)	MVCT Doses cGy (F)	OSLD vs Planned Dose % Difference (D-E)	OSLD vs MVCT Dose % Difference (D-F)	Planned vs MVCT Dose % Difference (E-F)
Left Femur Implant	Bladder 1	131.32	125.4	124	4.51	5.57	1.12	134.28	135	134	-0.54	0.21	0.74
	Bladder 2	141.99	136.04	134	4.19	5.63	1.50	159.05	139.48	139	12.30	12.61	0.34
	Bladder 3	121.32	116.56	115	3.92	5.21	1.34	142.04	129.32	128	8.96	9.88	1.02
	Bladder 4	155.1	138.56	136	10.66	12.31	1.85	166.24	143.24	143	13.84	13.98	0.17
	Bladder 5	122.51	117.28	115	4.27	6.13	1.94	138.36	127.32	126	7.98	8.93	1.04
	Bladder 6	115.71	116.4	116	-0.60	-0.25	0.34	147.41	127.28	127	13.66	13.85	0.22
	Bladder Wall 1	191.56	180.04	176	6.01	8.12	2.24	153.74	179.8	178	-16.95	-15.78	1.00
	Bladder Wall 2	181.8	180.2	177	0.88	2.64	1.78	195.06	180.16	179	7.64	8.23	0.64
	Bladder Wall 3	181.2	180.28	177	0.51	2.32	1.82	193.35	179.96	178	6.93	7.94	1.09
	Bladder Wall 4	181.34	180.04	175	0.72	3.50	2.80	184.09	180.32	179	2.05	2.76	0.73
	Bladder Wall 5	189.08	180.24	176	4.68	6.92	2.35	208.54	179.72	178	13.82	14.64	0.96
	Rectum Wall 1	184.65	181.8	177	1.54	4.14	2.64	191.85	181.16	178	5.57	7.22	1.74
	Rectum Wall 2	195.4	182.08	178	6.82	8.90	2.24	189.99	181.88	180	4.27	5.26	1.03
	Rectum Wall 3	194.68	183.04	179	5.98	8.05	2.21	190.1	182.76	180	3.86	5.31	1.51
	Rectum Wall 4	186.57	178.28	174	4.44	6.74	2.40	175.42	178.08	176	-1.52	-0.33	1.17
	Rectum Wall 5	174.44	181.36	177	-3.97	-1.47	2.40	186.6	181.16	179	2.92	4.07	1.19
	Rectum 1	156.63	148.36	144	5.28	8.06	2.94	146.6	149	147	-1.64	-0.27	1.34
	Rectum 2	162.23	148.16	145	8.67	10.62	2.13	146.5	148.76	147	-1.54	-0.34	1.18
	Rectum 3	157.3	152.04	149	3.34	5.28	2.00	159.72	153.36	151	3.98	5.46	1.54
	Rectum 4	159.63	150.84	148	5.51	7.29	1.88	157.8	152.48	150	3.37	4.94	1.63
	Rectum 5	164.4	153.88	150	6.40	8.76	2.52	146.62	153.76	151	-4.87	-2.99	1.80
Right Femur Implant	Bladder 1	111.82	117.96	116	-5.49	-3.74	1.66	123.1	122.2	121	0.73	1.71	0.98
	Bladder 2	117.6	140.4	138	-19.39	-17.35	1.71	140.2	136.8	135	2.43	3.71	1.32
	Bladder 3	140.5	116.64	115	16.98	18.15	1.41	127.8	117.76	117	7.86	8.45	0.65
	Bladder 4	137.42	141.96	140	-3.30	-1.88	1.38	142.4	137.92	136	3.15	4.49	1.39
	Bladder 5	130.22	126	125	3.24	4.01	0.79	128.59	130.92	130	-1.81	-1.10	0.70
	Bladder 6	159.12	119	116	25.21	27.10	2.52	130.6	119.88	119	8.21	8.88	0.73
	Bladder Wall 1	180.2	180.28	175	-0.04	2.89	2.93	188.1	180	178	4.31	5.37	1.11
	Bladder Wall 2	186.57	180.12	173	3.46	7.27	3.95	170.5	179.48	177	-5.27	-3.81	1.38
	Bladder Wall 3	130.84	180.16	175	-37.69	-33.75	2.86	186.32	179.88	178	3.46	4.47	1.05
	Bladder Wall 4	182.1	180.08	176	1.11	3.35	2.27	184.25	180.04	178	2.28	3.39	1.13
	Bladder Wall 5	186.9	180.24	175	3.56	6.37	2.91	183	180.16	178	1.55	2.73	1.20

Contd...

Supplementary Table: Contd...

Case	Position	IM_No_Res						IM_Exit Only					
		OSLD Doses cGy (A)	Planned (TPS) Doses CGy (B)	MVCT Doses cGy (C)	OSLD vs Planned Dose % Difference (A-B)	OSLD vs MVCT Dose % Difference (A-C)	Planned vs MVCT Dose % Difference (B-C)	OSLD Doses cGy (D)	Planned (TPS) Doses CGy (E)	MVCT Doses cGy (F)	OSLD vs Planned Dose % Difference (D-E)	OSLD vs MVCT Dose % Difference (D-F)	Planned vs MVCT Dose % Difference (E-F)
	Rectum Wall 1	131.32	125.4	124	4.51	5.57	1.12	172.7	180.4	177	-4.46	-2.49	1.88
	Rectum Wall 2	185.1	180.36	175	2.56	5.46	2.97	188.8	182.12	179	3.54	5.19	1.71
	Rectum Wall 3	177.98	180.28	175	-1.29	1.67	2.93	184.7	180.72	178	2.15	3.63	1.51
	Rectum Wall 4	187.53	180.48	176	3.76	6.15	2.48	184.8	179.76	177	2.73	4.22	1.54
	Rectum Wall 5	183.9	182.04	176	1.01	4.30	3.32	193.6	182.72	179	5.62	7.54	2.04
	Rectum 1	162.14	158.68	154	2.13	5.02	2.95	147.4	151.84	149	-3.01	-1.09	1.87
	Rectum 2	161.5	155.92	152	3.46	5.88	2.51	158.7	152.24	150	4.07	5.48	1.47
	Rectum 3	171.43	164.4	160	4.10	6.67	2.68	158.33	149.64	148	5.49	6.52	1.10
	Rectum 4	161.25	162.88	159	-1.01	1.40	2.38	160.5	149.68	148	6.74	7.79	1.12
	Rectum 5	155.4	154.52	150	0.57	3.47	2.93	156.1	149.76	147	4.06	5.83	1.84
Bilateral Femur Implant	Bladder 1	137.62	122.92	121	10.68	12.08	1.56	135.6	134.52	134	0.80	1.18	0.39
	Bladder 2	142.1	134	131	5.70	7.81	2.24	144.4	138.68	137	3.96	5.12	1.21
	Bladder 3	131.98	119.88	117	9.17	11.35	2.40	135	128.68	128	4.68	5.19	0.53
	Bladder 4	147.36	135.76	132	7.87	10.42	2.77	143.9	140.76	139	2.18	3.41	1.25
	Bladder 5	130.14	122.72	121	5.70	7.02	1.40	150.7	137.04	137	9.06	9.09	0.03
	Bladder 6	99.506	117.36	116	-17.94	-16.58	1.16	139	122.36	122	11.97	12.23	0.29
	Bladder Wall 1	162.71	179.68	173	-10.43	-6.32	3.72	197.7	176.8	182	10.57	7.94	-2.94
	Bladder Wall 2	180.72	179.72	171	0.55	5.38	4.85	194.5	179.68	179	7.62	7.97	0.38
	Bladder Wall 3	136.53	179.84	172	-31.72	-25.98	4.36	192.6	178.12	181	7.52	6.02	-1.62
	Bladder Wall 4	185.11	179.72	171	2.91	7.62	4.85	191.5	179.24	179	6.40	6.53	0.13
	Bladder Wall 5	193.86	180.2	173	7.05	10.76	4.00	188.6	178.8	183	5.20	2.97	-2.35
	Rectum Wall 1	193.03	180.48	174	6.50	9.86	3.59	173.6	180.36	179	-3.89	-3.11	0.75
	Rectum Wall 2	191.11	182.32	176	4.60	7.91	3.47	195.7	182.08	181	6.96	7.51	0.59
	Rectum Wall 3	189.51	180.76	174	4.62	8.18	3.74	195.5	180.36	179	7.74	8.44	0.75
	Rectum Wall 4	186.82	179.96	175	3.67	6.33	2.76	197	180.8	180	8.22	8.63	0.44
	Rectum Wall 5	186.53	182.48	146	2.17	21.73	19.99	187	181.88	180	2.74	3.74	1.03
	Rectum 1	143.33	151.96	147	-6.02	-2.56	3.26	153.4	150.2	149	2.09	2.87	0.80
	Rectum 2	156.54	151	145	3.54	7.37	3.97	164.3	152.44	151	7.22	8.09	0.94
	Rectum 3	147.79	149.8	131	-1.36	11.36	12.55	153.4	149.44	148	2.58	3.52	0.96
	Rectum 4	148.6	150.8	146	-1.48	1.75	3.18	158	149.68	148	5.27	6.33	1.12
	Rectum 5	145.53	149.96	146	-3.04	-0.32	2.64	149.8	149.6	148	0.13	1.20	1.07

MVCT: Megavoltage computed tomography, OSL: Optically stimulated luminescence, TPS: Treatment planning system